Artıbilim: Adana Alparslan Türkeş Bilim ve Teknoloji Üniversitesi Fen Bilimleri Dergisi 4(2), Aralık 2021, 24-43
Adana Alparslan Turkes Science and Technology University Journal of Science

Controlability of multi-rotors under motor fault effect

Davood Asadi [*1], Karim Ahmadi[1], Seid Yaser Nabavi[1], Önder Tutsoy[2]

[1] Adana Alparslan Türkeş Bilim ve Teknoloji Üniversitesi, Havacılık ve Uzay Bilimleri Fakültesi, Havacılık ve Uzay Mühendisliği Bölümü, Adana, *ORCID: 0000-0002-2066-6016, 0000-0002-2633-3351, 0000-0003-1836-2600*
[2] Adana Alparslan Türkeş Bilim ve Teknoloji Üniversitesi, Mühendislik Fakültesi, Elektrik ve Elektronik Mühendisliği Bölümü, Adana, *ORCID: 0000-0003-2556-2002*

Geliş Tarihi:17.11.2021 **Kabul Tarihi:**27.11.2021

Abstract

The multi-rotor unmanned aerial vehicles (UAVs) are being increasingly applied in both military and civil applications. Motor fault or failure is a common type of fault on multi-rotors, which might take place during mission and operation. Various configurations of fault are considered regarding the desired faulty motor in multi-rotors including the quadcopters and hexarotors. The existence of fault on different motors can lead to different controllability around the vehicle's body axes. Here, configurations mean the rotation angle of the multi-rotor's body axes respecting the fault or failure on the arbitrary motor of the multi-rotor. Therefore, it is essential to know which configuration has better reliability in the presence of motor faults or failures. Since the multirotor's reliability and recoverability is highly related to its controllability, the controllability gramian approach, which is derived from the linear systems theory, as a control objective. The eigenvalues of the controllability gramian can be used as a surrogate for the energy required to control the corresponding eigenvector. Accordingly, the results clearly demonstrate the effect of motor fault on multi-rotor controllability. Additionally, in this paper, configurations with minimum required energy are introduced for quadrotors and hexarotors in different motor faults and failures.

Keywords: Controllability, Motor fault, Multi-rotor

Motor hata etkisi altında multikopterlerin kontrol edilebilirliği

Özet

Multikopter insansız hava araçları (İHA) hem askeri hem de sivil uygulamalarda giderek daha fazla kullanılmaktadır. Motor arızası veya kaybı, görev ve operasyon sırasında meydana gelebilecek multikopterlerde yaygın bir arıza türüdür. Quadcopters ve hexarotors dahil olmak üzere multikopterlerde arızalı motorla ilgili çeşitli arıza konfigürasyonları göz önünde bulundurulur. Farklı motorlarda arıza bulunması, aracın gövde eksenlerinde farklı kontrol edilebilirliklere yol açabilir. Burada konfigürasyonlar, multikopterin keyfi motorundaki arızaya göre multikopterin gövde eksenlerinin dönüş açısı anlamına gelir. Bu nedenle, motor arızalarının varlığında hangi konfigürasyonun daha iyi güvenilirliğe sahip olduğunu bilmek önemlidir. Multikopterin güvenilirliği ve kurtarılabilirliği, kontrol edilebilirliği ile büyük ölçüde ilişkili olduğundan, bir kontrol hedefi olarak doğrusal sistemler teorisinden türetilen kontrol edilebilirlik gramian yaklaşımı. Kontrol edilebilirlik gramianının özdeğerleri, karşılık gelen özvektörü kontrol etmek için gereken enerji için bir vekil olarak kullanılabilir. Buna göre, sonuçlar motor arızasının multikopter kontrol edilebilirliği üzerindeki etkisini açıkça göstermektedir. Ek olarak, bu yazıda, farklı motor arızalarında quadrotor ve hexarotors için minimum gerekli enerjiye sahip konfigürasyonlar tanıtılmaktadır.

Anahtar Kelimeler: Kontrol edilebilirlik, Motor arızası, Multikopter

[*]Sorumlu yazar (Corresponding author): Davood Asadi, dasadihendoustani@atu.edu.tr.
Künye Bilgisi: Asadi, D., Ahmadi, K., Nabavi, S.Y., Tutsoy, Ö. (2021). Controlability of Multi-rotors under Motor Fault Effect. Artıbilim: Adana Alparslan Türkeş Bilim ve Teknoloji Üniversitesi Fen Bilimleri Dergisi, 4(2), 24-43.

1. Introduction

The application of multi-rotor unmanned aerial vehicles (UAVs) has been considerably increased in outdoor and indoor environments due to their significant advantages such as low cost, compactness, and maneuverability. This fast development raises the unsolved problem of safety and reliability for the UAVs [1, 2]. Motor fault or failure is a viable problem on multi-rotor UAVs, which can lead in to crash, costly damages to the UAV, and endanger the facilities or human on the ground [3, 4]. Thus, fault-tolerant strategies like fault-tolerant control algorithms and multi-rotors with fault-tolerant configurations has widely attracted the researchers' attention [5, 6]. Both strategies can assist the control recovery of the multi-rotor in case of motor fault or failure.

As the first strategy, fault-tolerant control techniques have been proposed in several researches to recover the control of the faulty aircraft [7-12]. Nonlinear L1 adaptive control [7], robust adaptive control [8], adaptive sliding mode control [9], Linear Parametric Variable (LPV) sliding mode control [10], optimal adaptive control [11], and Model Reference Adaptive Control (MRAC) [12] are some instances of direct fault-tolerant control algorithms. In addition to the direct methods, fault-detection and identification algorithms are also used in some references in the fault-tolerant control strategy [13]. Timely detection of the actuator failures and estimation of its severity play an important role in avoiding crashes and leading to fast recovery for a safe landing. Fault-detection approaches can be categorized into model-based, signal-based, knowledge-based, and active diagnosis techniques [14]. Ref. [15] proposed a two-stage Kalman filter to detect, isolate, and estimate possible faults in each motor whereas the method was evaluated on a UAV testbed. In Ref. [16], an adaptive Thau observer was developed to estimate and detect the actuator faults. A parity space method with recursive least squares algorithm was introduced in [17], for actuator faults detection and identification of a drone.

Another strategy regarding multi-rotors is to have a fault-tolerant configuration. Since different configurations can be considered for multi-rotors, introducing a configuration with higher reliability in the presence of motor faults or failures is more preferable [18]. The reliability of multi-rotors in presence of fault is highly dependent on the existing energy to control the flying vehicle, which necessitates defining a measure of fault recoverability. To investigate the recoverability condition, the controllability gramian of the system can be applied [19]. The controllability gramian W_c is a matrix that can be used to check the level of controllability. Controllability gramian is used as a measure for the energy required to control the corresponding eigenvector. The corresponding eigenvalues can thus be considered as a representative for controlling a given state-space variable. Higher eigenvalue determines lower energy required to control the system along that eigenvector direction [19, 20].

There are various conventional configurations such as quadcopters, hexarotors, and octocopters. Different configurations lead to different flight characteristics. Conventional configurations include standard symmetric configurations and nonstandard configurations. Various unconventional configurations have been proposed in the literature. Variable center of gravity configuration [21], variable motor angle, blade variable pitch angle [22], sliding arm configuration [23], and triangular quadrotor configuration [24] are some instances of unconventional configurations, which have been reported in the literature. A new configuration of fixed-pitch multi-rotor that combines the energy efficiency of a helicopter and the mechanical simplicity of a quadcopter is proposed in [24]. In [25], a design optimization process of multi-rotors with different configurations was presented, and the optimal goals focus on the dynamic performance and the flight time. Although some research has studied the optimization problem of multi-rotor configuration, the optimal choice of configuration based on flight reliability remains an open problem.

Controlability of multi-rotors under motor fault effect

This paper concentrates on conventional standard configurations of multi-rotors including the quadrotor and the hexarotor. Quadrotors cannot retain controllability in presence of one or more rotors failure and changes to an under-actuated system. In the case of motor failure, reduced attitude including the roll and pitch angle is retained and yaw control is lost, therefore, the quadrotor starts turning around the yaw axis [26, 27]. Another interesting platform, which seems to be more robust respecting motor failure is hexarotor. Despite the higher numbers of motors with respect to quadrotors, researchers demonstrated that symmetric hexarotors are not fully controllable in case of one motor failure, in which yaw control is lost if one engine is failed [28]. In the literature, hexarotors with tilted rotors are proposed to improve controllability after motor failure [29]. Although asymmetric multi-rotor configurations have been examined in several researches, most commercial and ready platforms rely on symmetric configurations. In fact, it is difficult to reach a controller that can cope with motor failures in the standard configurations, and most proposed controller algorithms in the literature are confined to reduced attitude control [30]. Therefore, introducing more reliable multi-rotor configurations with more controllability characteristics in presence of motor fault and failure would be a logical approach. Due to the characteristics of multi-rotors, rotors can only provide unidirectional lift (upward or downward) in practice, hence, classical controllability theories of linear systems are insufficient to test the controllability of multi-rotors. Although the linear controllability theory is not applicable to multi-rotors, the magnitude of eigenvalues can be a surrogate of the required energy to move the vehicle in a specific direction.

Motivated by the above discussion, this paper explores the standard multi-rotor configuration to find the optimal configuration addressing motor fault and failure. The effect of different rotation angles of body for various magnitudes of motor faults and failures on the system controllability gramian is investigated. Accordingly, the magnitudes of eigenvalues of the controllability gramian, which represent the controllability and the required energy to move the system around the specific direction, are computed. In our approach, the rotation angle with a minimum difference of controllability around the body axes (roll and pitch directions of multi-rotor) is introduced as the best configuration, which can retain controllability after a motor fault. As far as the authors know, the presented analysis and results have not been investigated or presented before in the literature.

The remainder of the paper is organized as follow. First, the dynamic equations of the model are presented and the linearized model corresponding to body rotation angle is derived. Next, the controllability theory and its application to our desired problem are described. Finally, the results and analysis of different fault combinations are presented for different configurations of multi-rotor.

2. Dynamic equations and linearization

The translational and rotational equations of the quadrotor in the body frame are presented in Eqs. (1), respectively [2, 11]. As depicted in Figure 1 and 2, the quadrotor consists of four motors. Number one and three motors rotate counter-clockwise with velocities Ω_1, Ω_3, respectively, whereas the other two motors (number 2 and 4) rotate in the opposite (clockwise) direction with velocities Ω_2, Ω_4.

Figure 1. S500 quadrotor

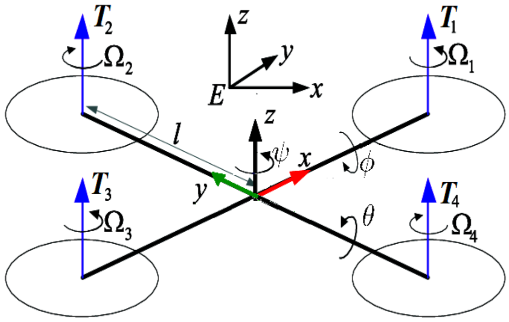

Figure 2. Schematic representation of quadrotor

Applying the rigid-body equations of motion and Euler angle transformation (Eq. (1)), the complete dynamical model of the quadrotor is presented as below:

$$\begin{aligned} \ddot{z} &= -g + (cos\theta\ cos\varphi)\frac{u_z}{m} \\ \dot{p} &= \frac{I_{yy} - I_{zz}}{I_{xx}} qr + \frac{u_\varphi}{I_{xx}} \\ \dot{q} &= \frac{I_{zz} - I_{xx}}{I_{yy}} pr + \frac{u_\theta}{I_{yy}} \\ \dot{r} &= \frac{I_{yy} - I_{zz}}{I_{xx}} qr + \frac{u_\psi}{I_{zz}} \end{aligned} \tag{1}$$

where z is the position of multi-rotor center of mass in inertial frame and θ, φ are pitch and roll angles, which represent the body frame rotation with respect to the inertial frame. I_{xx}, I_{yy}, and I_{zz} are the moments of inertia in x, y, and z body direction, respectively, m is the system mass, and g is the gravitational acceleration. The quadrotor inputs are represented by $u_z, u_\varphi, u_\theta, u_\psi$, which are the total lift force (u_z) generated by propellers in z-direction and moments about x, y, z axes, respectively.

Depending on the multi-rotor configuration and the number of motors (quadrotor or hexarotor), the force and moment control inputs can change. This paper assumes number one motor is in the x-body direction, therefore, rotations of motor number one corresponding the x-body axis is shown by α angle. Different configurations can be considered. According to Figure 3, the extended control inputs for the case of quadrotor and hexarotor are presented below:

A. In case of quadrotor

$$\begin{aligned} u_z &= T_1 + T_2 + T_3 + T_4 \\ u_\varphi &= l(-T_1 \sin\alpha + T_2 cos\alpha + T_3 \sin\alpha - T_4 cos\alpha) \\ u_\theta &= l(-T_1 \cos\alpha - T_2 sin\alpha + T_3 \cos\alpha + T_4 sin\alpha) \\ u_\psi &= k(T_1 + T_3 - T_2 - T_4) \end{aligned} \tag{2}$$

B. In case of hexarotor

$$\begin{gathered} u_z = T_1 + T_2 + T_3 + T_4 + T_5 + T_6 \\ u_\varphi = l\left(-T_1 \sin\alpha + T_2 \sin\left(\frac{\pi}{3} - \alpha\right) + T_3 \cos\left(\frac{\pi}{6} - \alpha\right) + T_4 \sin\alpha - \sin\left(\frac{\pi}{3} - \alpha\right) - \sin\left(\frac{\pi}{3} + \alpha\right)\right) \\ u_\theta = l(-T_1 \cos\alpha - T_2 \cos\left(\frac{\pi}{3} - \alpha\right) + T_3 \sin\left(\frac{\pi}{6} - \alpha\right) + T_4 \cos\alpha + \cos\left(\frac{\pi}{3} - \alpha\right) - \cos\left(\frac{\pi}{3} + \alpha\right)) \\ u_\psi = k(T_1 + T_3 + T_5 - T_2 - T_4 - T_6) \end{gathered} \quad (3)$$

Where T_i is the thrust force of the ith motor, l is the moment arm (C.G to motor distance), k is a constant related to motor drag, and α is the rotation angle of multi-rotor respecting the reference body axis related to the plus configuration, as shown in Figure 3.

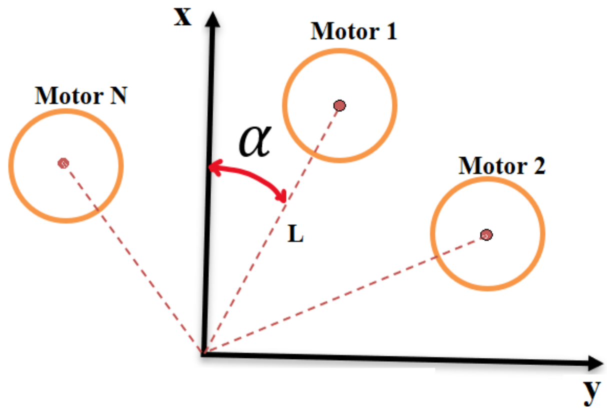

Figure 3. Multi-rotor rotation in body axes

To reach the linear state space model of the system ($\dot{X} = AX + Bu$), nonlinear equation (Eq. 1) is linearized around the hover flight condition. Accordingly, assuming the system states as $X = (\dot{z}, p, q, r)$, the state and control matrices are derived for two cases of quadcopter and hexacopter:

1- In case of quadrotor

$$A = \begin{bmatrix} 0 & 0 & 0 & 0 \\ 0 & 0 & 0 & 0 \\ 0 & 0 & 0 & 0 \\ 0 & 0 & 0 & 0 \end{bmatrix}, \quad B = \begin{bmatrix} 1/m & 1/m & 1/m & 1/m \\ -l\sin\alpha/I_x & l\cos\alpha/I_x & l\sin\alpha/I_x & -l\cos\alpha/I_x \\ -l\cos\alpha/I_y & -l\sin\alpha/I_y & l\cos\alpha/I_y & l\sin\alpha/I_y \\ k/I_z & -k/I_z & k/I_z & -k/I_z \end{bmatrix} \quad (4)$$

2- In case of hexarotor

$A = [0]_{6\times6}$

$$B = \begin{bmatrix} 1/m & 1/m & 1/m & 1/m & 1/m & 1/m \\ -l\sin\alpha/I_x & l\sin(\frac{\pi}{3} - \alpha)/I_x & l\cos(\frac{\pi}{6} - \alpha)/I_x & l\sin\alpha/I_x & -l\sin(\frac{\pi}{3} - \alpha)/I_x & -l\sin(\frac{\pi}{3} + \alpha)/I_x \\ -l\cos\alpha/I_x & -l\cos(\frac{\pi}{3} - \alpha)/I_x & l\sin(\frac{\pi}{6} - \alpha)/I_x & l\cos\alpha/I_x & -l\cos(\frac{\pi}{3} - \alpha)/I_x & -l\cos(\frac{\pi}{3} + \alpha)/I_x \\ k/I_z & -k/I_z & k/I_z & -k/I_z & k/I_z & -k/I_z \end{bmatrix} \quad (5)$$

By application of the above linear model, the controllability and the existing energy to control the multirotor around each axis will be examined in the following.

3. Controllability of multi-rotors

According to classical control theories, a controllability matrix can be used to determine the controllability of the system. The full rank controllability matrix determined a fully controllable system corresponding to the selected states of the system. Despite many control systems in which the actuators generally act in both directions (positive and negative directions), multi-rotors just generate unidirectional lift (upward). Therefore, classical controllability theories of linear systems cannot be applied to control the system's controllability. In fact, the controllability gramian or controllability matrix cannot support the judgment about the system controllability. There are several researches, which have applied different techniques to examine the controllability of unidirectional systems [31-33], in which different configurations of multi-rotors are analyzed to determine whether the desired system is fully controllable or not. Respecting the controllability of standard quadrotors, it is known that failure of one engine results in an uncontrollable system. Controllability of other standard multirotors including the hexarotors and octarotors depends on engine rotation configuration and the faulty rotor. According to the literature, as shown in Figure 4, two different configurations can be considered for the hexarotor (not quadrotor) based on the direction of the rotor-turn.

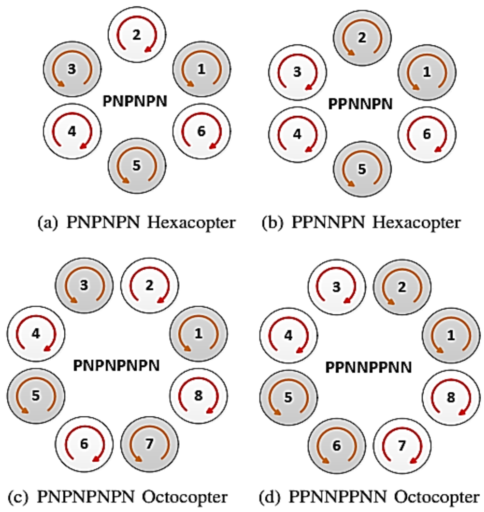

Figure 4. Hexarotor and octarotor with traditional arrangement of rotors and non-standard rotors

According to the results [31], the controllability of the standard rotations (PNPNPN) of hexarotor loses full rotational controllability around all three directions of body axes and degrades to just pitch and roll controllability in case of one rotor failure. The non-standard configuration (PPNNPN) is maintaining its full controllability in 33% of up to two random motor failures, which determines the fault-tolerant capabilities of the non-standard configuration. In addition, in 71% of up to two random motor lost configurations are controllable in pitch and roll directions [28, 31]. Similar results can be derived for octorotors, which have full controllability in 78% of two random motor failures as well as pitch-roll controllability in all cases of up to two motor failures for the traditional case (PNPNPNPN). For the non-traditional octorotors (PPNNPPNN) this value increases to 89%. Although the non-standard configuration is more fault-tolerant but its performance is less than the standard configuration in terms of moment-producing capabilities. Therefore, changing the rotor turn direction and arrangement is a tradeoff between performance and fault tolerance, although the performance degradation is rather small [31].

3.1. Controllability gramian

This paper applies the controllability gramian and its eigenvalues to specify the level of controllability in each specific direction of eigenvectors for different configurations and motor faults and failures. Based on the eigenvalues, the minimum difference of controllability will be introduced as the desired configuration. The linear state-space model of the quadcopter can be written as:

$$\dot{x} = Ax + Bu \\ y = Cx + D \tag{6}$$

If there exists a control input *u(t)*, which can derive the system from an initial state x_0 at time t_0 to a final state x_f at time t_f, the system is called controllable. The controllability gramiam matrix W_c, can be applied to determine the controllability of the multi-rotor. The controllability gramian of the time-invariant linear system based on matrices *A* and *B* is defined as:

$$W_c(t_0, t_f) = \int_{t_0}^{t_f} e^{A\tau} BB^T e^{A^T\tau} d\tau \tag{7}$$

The introduced controllability gramian is used to generate the control law with least amount of energy, which will transfer the system from the initial state x_0 at t_0 to the final state x_f at time t_f.

$$u(t) = -B^T e^{A^T(t_0-t)} W_c^{-1}(t_0, t_f)\, x_0 \tag{8}$$

Based on the above control input *u(t)*, the minimum energy control can be written as:

$$\int_{t_0}^{t_f} \|u(t)\|^2\, dt = x_0^T W_c^{-1}(t_0, t_f) x_0 \tag{9}$$

The eigenvalues (λ_i) of W_c can be considered as a metric in terms of energy along the specific directions (x_i). Accordingly, the specific direction are the eigenvectors corresponding to the eigenvalues as below:

$$W_c X_i = \lambda_i X_i \tag{10}$$

Where λ_i are the eigenvalues of W_c and X_i are the corresponding eigenvectors. Higher magnitudes of eigenvalues λ_i specify lower required energy to move in the direction X_i [34]. In fact, the magnitude of the eigenvalue quantifies the required energy to move the system in different directions of the state space, which are specified by the eigenvectors of W_c. The eigenvalues of the controllability gramian change in presence of engine fault or failure on multi-rotor. Depending on the location of the fault (which motor), the magnitude of the related eigenvalues around each direction changes. According to Eq. 1 for the linearized model of the multirotor, controllability gramian is a 4×4 matrix, with 4 eigenvalues. One eigenvalue is related to controllability in z direction (thrust direction), the other three ones are eigenvalues corresponding to rotations around roll, pitch, and yaw. According to Figure 3, by rotating the multi-rotor body axes with alpha angle around the *z* axes, the eigenvalues around roll and pitch axes change but the eigenvalues related to force equation in *z* direction and the yawing moment are unchanged. It means that, by having the same magnitude of fault on motor number 1 and 2, the eigenvalues related to the pitch and roll axes changes but in the direction of thrust force and yawing moment are unchanged. Therefore, the control objective is selected in the following form:

$$J = (|\lambda_{Roll}| - |\lambda_{Pitch}|)^2 \tag{11}$$

Analyzing the controllability around the main axes of the multirotor determines the direction with maximum controllability. Additionally, by application of cost function of Eq. 11, compromise directions with minimum difference of controllability are derived for different engine failures. In fact, the main objective in this paper is to find the main directions in the *x-y* plane of the multi-rotor in which the controllability around the main axes has a minimum difference in presence of motor faults and failure. In the following different configurations and various faults are considered for two cases of quadrotor and hexarotor.

4. Controllability analysis

For a quadrotor with plus configuration, state matrix and input matrices are derived. The matrices *A* and *B* are according to Eq. 4. According to Figure (3), when α is zero, the multirotor is in plus configuration. The system states are *Vz*, *p*, *q*, *r* accordingly. Therefore, in the eigenvalue and eigenvector matrix, the first element determines the controllability in z direction (channel 1), the second element is related to pitch (channel 3), and the third and fourth are related to roll (channel 2) and yaw (channel 4). When α is zero two motors have main controllability around pitch (channel 3) and two other motors have the main controllability around the roll (channel 2). By increasing the α which is the rotation of body x-axes, the two motors which have controllability around the second channel will have controllability around the third channel two. Therefore, at different values of α two motors have main controllability and the two other ones are having a coupling of controllability. The controllability in the first and forth channel is unaffected by motor fault. Based on the above discussions, the following parameters related to controllability around the roll and pitch channels are defined:

$\mathbf{US_{21}}$: Controllability measure due to the motors with most effect around roll axes (channel 2)

$\mathbf{US_{22}}$: (Coupling) controllability measure of the $\mathbf{US_{21}}$ motors around the pitch axes (motors with most effect around roll axes generate a coupling controllability around pitch axes)

$\mathbf{US_{32}}$: Controllability measure due to the motors with most effect around pitch axes (channel 3)

$\mathbf{US_{31}}$: (Coupling) controllability measure of the $\mathbf{US_{32}}$ motors around the roll axes (motors with most effect around pitch axes generate a coupling controllability around roll axes)

Corresponding to the above parameters derived from the eigenvalues and eigenvectors of the multirotor as well as considering the cost function introduced in Eq. 11, the following criteria is defined as the cost function:

Criteria: minimum difference between: the main controllability around roll axes and pitch axes and the coupling around roll and pitch axes:

$$J = (|\boldsymbol{US_{21}}| - |\boldsymbol{US_{32}}|)^2 + (|\boldsymbol{US_{31}}| - |\boldsymbol{US_{22}}|)^2 \quad (12)$$

4.1. Quadrotor controllability analysis

This section examines the controllability of the quadrotor in case of one rotor failure and in different rotation angles of α. The goal is to specify the optimum angle with minimum magnitude of J. As the first illustration, the variation of the parameters $\mathbf{US_{21}}$, $\mathbf{US_{22}}$, $\mathbf{US_{32}}$, $\mathbf{US_{31}}$ are shown for the quadrotor with no rotor failure. In this case, the controllability matrix is of full rank and therefore controllable. Figure 5*a* illustrates the variations of the parameters and Figure 5*b* show the difference of controllability according to Eq. 12. Accordingly, for a quadrotor with no rotor failure the variation is equal to zero for all angles. Thus, body rotation has no effect on the controllability parameters of quadrotor around the main axes.

Fault and failure effect on the controllability of quadrotor has been illustrated in Fig 5(*c-f*). In case of quadrotor, if one motor is out (failure), rank of controllability gramian is 3, which means loss of control around the *z* axis. In case of two motor failures, the system rank is 2. Accordingly, Fig 5 (*c*, *d*) illustrates the effect of 50% of fault on number one rotor and Fig 5 (*e*, *f*) depicts the effect of failure of number one motor. Accordingly, the minimum difference of controllability takes place at the rotation angle of 45.

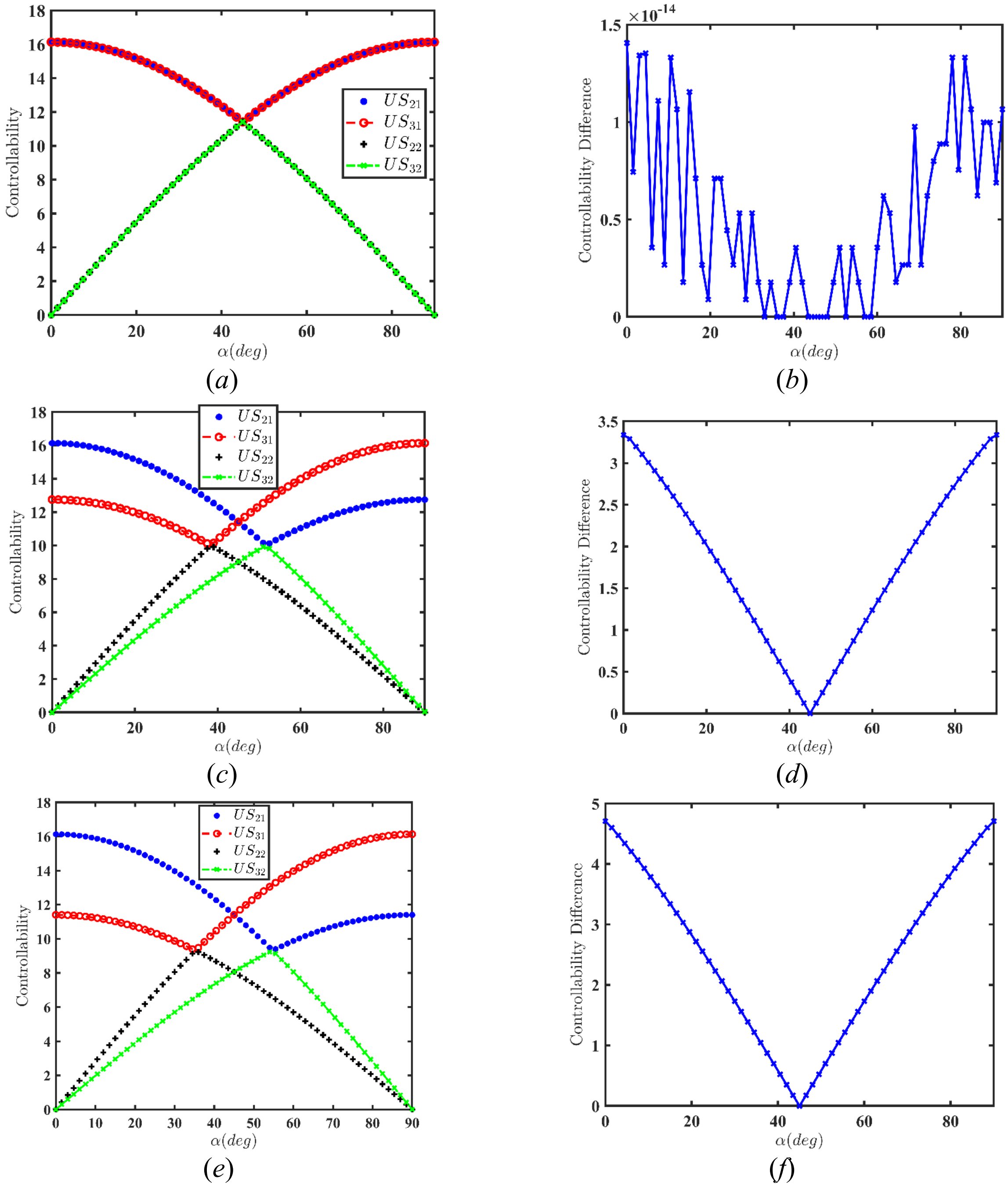

Figure 5. Variation of controllability parameters and the controllability difference *(J) for quadrotor (a, b) No rotor failure, (c, d) 50% fault on rotor number 1, (e, f) failure on rotor number one*

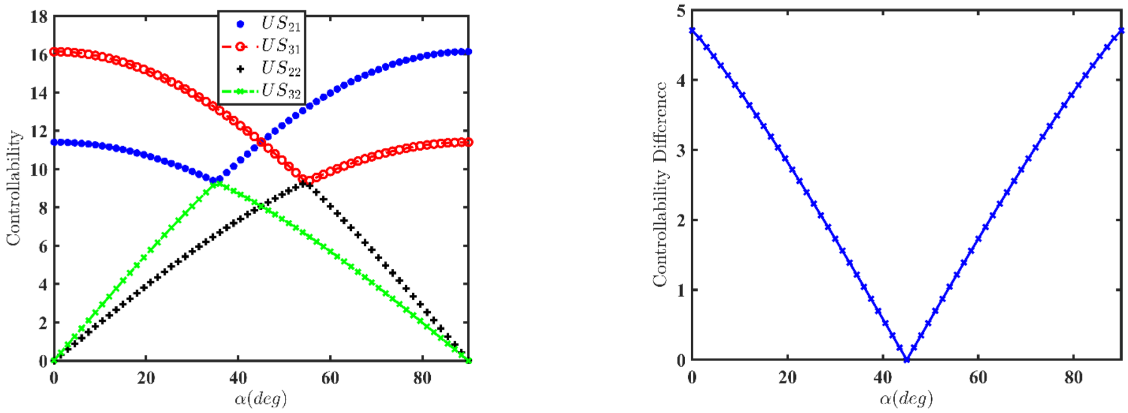

(*a*) (*b*)

Figure 6. Failure of number two motor

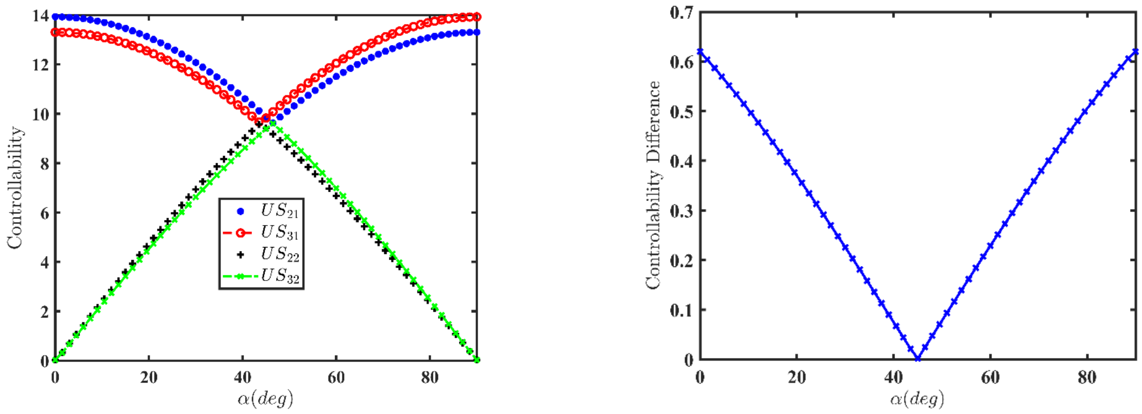

(*a*) (*b*)

Figure 7. 40% of fault on number one rotor and 30% of fault on number two motor

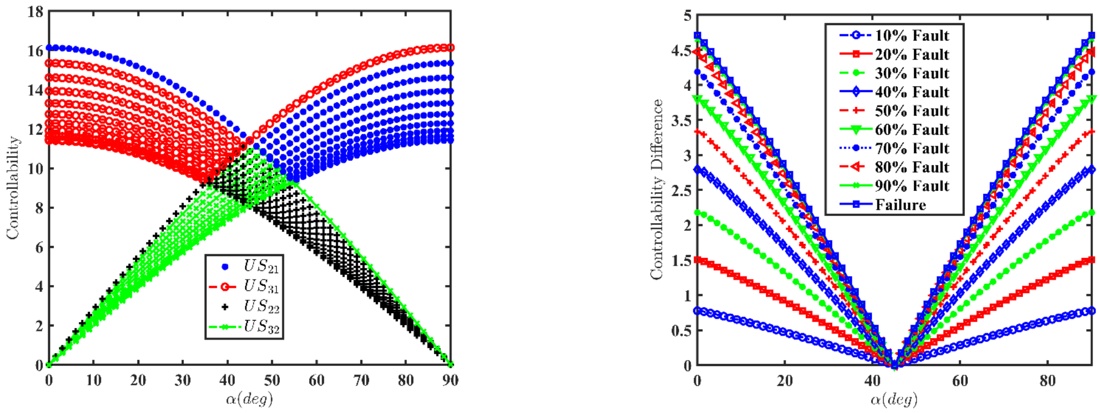

Figure 8. Different magnitudes of fault on number two motor

Figure 6 shows the effect of failure of number 2 motor on the system controllability and the cost function while Figure 7 illustrates the effect of composition of faults of number one and number two rotors. Figure 8 illustrates the Effect of the magnitude of fault on number two rotor. For all variations of engine fault, with one motor or two motors, the angle with minimum difference of controllability around the body axes is 45 degrees and does not change with magnitude of fault and engine fault configuration. According to the above results, the quadrotor with 45 degrees of rotation is known as cross configuration. In addition to the above benefit for cross-configuration of quadrotors respecting the plus configuration, the following advantages can also be expressed for the cross configuration.

4.2. Hexarotor analysis

The same analysis as above will be executed for the hexarotor airframe. In addition to the rotation angle, different fault and failures are considered on different motors. Figure 9 (*a-f*) represents the controllability and the difference of controllability around the pitch and roll axes for no fault, 50% of fault, and the failure of number one motor. Accordingly, for different magnitudes of fault or failure on number one rotor, $\alpha = 45°$ represents the optimum body rotation angle. The optimum angle for number two rotor failure is $\alpha = 15°$ and for number three is $\alpha = 75°$, respectively, according to Figures (10, 11). For simultaneous failure of two rotors, $\alpha = 75°$ for failures of number one and two rotors, $\alpha = 45°$ for failures of number two and three rotors, $\alpha = 15°$ for failures of number three and four rotors, $\alpha = 45°$ for failures of number one and four rotors, and $\alpha = 15°$ for failures of number one and four rotors, respectively according to Figures (13-16). Figure (17) illustrate simultaneous faults on three rotors. For failure of number one, three, and six $\alpha = 0°$ shows the minimum angle. Figures (18-21) illustrate the effect of different magnitudes of faults on different rotors. Accordingly, for different faults on number one motor $\alpha = 45°$, for number two motor $\alpha = 15°$ are the minimum values for the controllability difference. As shown in Figures (20, 21) different faults on simultaneous faults on two rotors result in different minimum angles.

For quadrotors in which the optimum configuration always takes place on $\alpha = 45°$ that is not dependent on the magnitude of the fault and the failure as well as the number of faulty rotors. Despite quadrotors, the magnitude of fault and the number of faulty rotors affects the angle with minimum controllability difference. In fact, in hexarotor, by changing the magnitude of fault on one rotor, two rotors, and three rotors configuration, the minimum angle changes depending on the magnitude and the number of faulty motors. If the magnitudes of faults on motors are different, the variation changes the minimum point and it shifts to left or right depending on the magnitude of fault on the rotors.

Based on the symmetrical configuration of hexarotor, the results of different magnitudes of faults or failures on some rotors are similar to each other. As some instances:

- The results of failure on motor four are the same as failures on motor one.
- The results of failure on motor five are the same as failures on motor two.
- The results of failure on motor six are the same as failures on motor three.
- The results of failure on motor four and five are the same as failures on motor one and two.
- The results of failure on motor five and six are the same as failures on motor two and three.
- The results of failure on motor three and four are the same as failures on motor six and one.
- The results of failure on motor one and three are the same as failures on motor four and three.
- The results of failure on motor one and five are the same as failures on motor one and two.
- The results of failure on motor two and five are the same as failures on motor three and six.

The above analysis can help the selection of the best configuration based on the fault of failure of the rotor. Fault detection algorithm inside the flight control system can determine the magnitude of the fault of existence of the failure on the rotor. Based on the detected fault or failure, the controller can select a suitable strategy for the continuation of the flight. In one strategy, the controller can rotate the body axes according to the calculated optimum angles and then continue the flight toward the landing area. In this strategy, the controllability of multirotor around the main axes of pitch and roll are having the minimum difference. Therefore, the continuation of flight with this strategy will provide controllability around both axes and can increase flight safety.

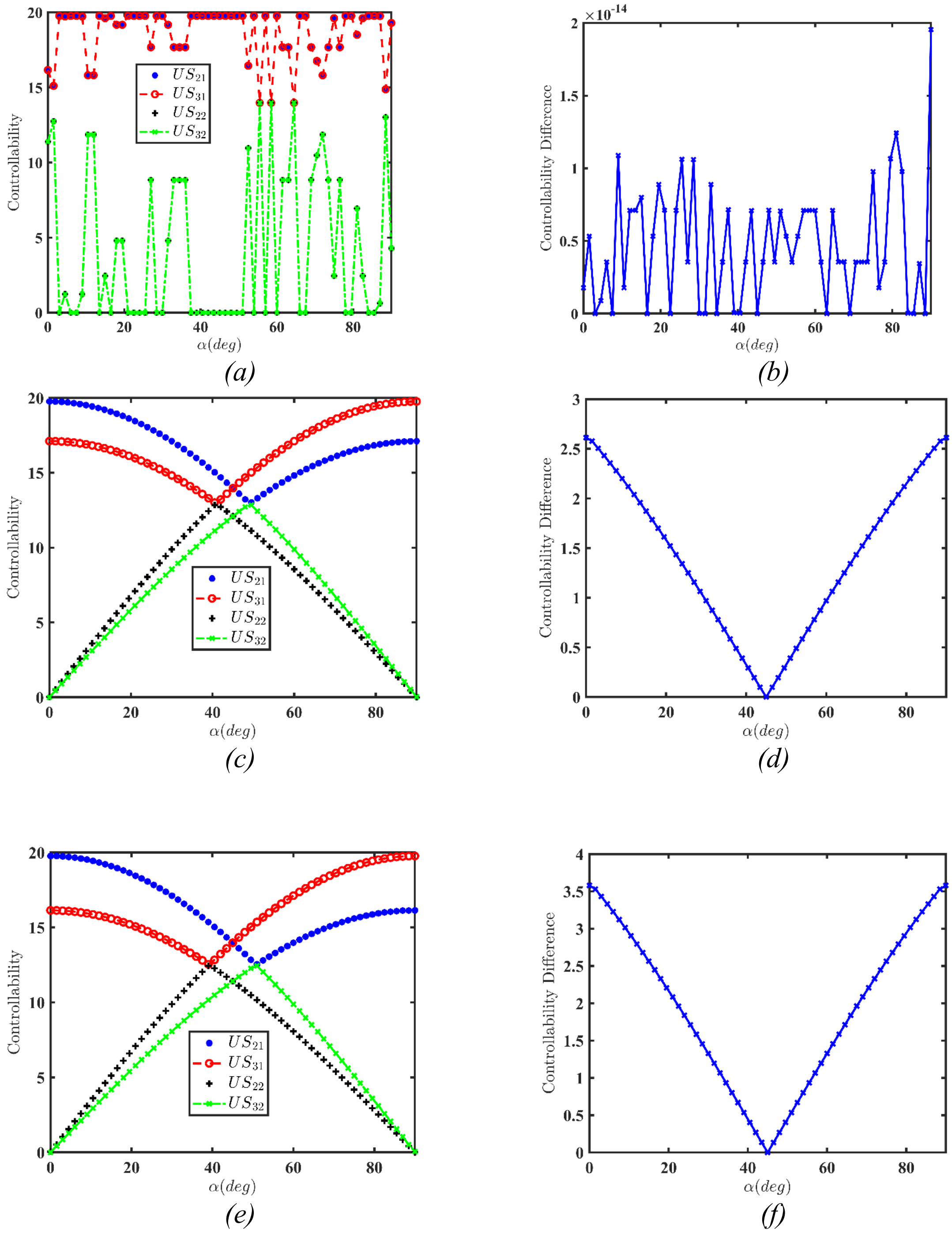

Figure 9. Variation of controllability parameters and the controllability difference *(J) for quadrotor (a, b) No rotor failure, (c, d) 50% fault on rotor number 1, (e, f) failure on rotor number one*

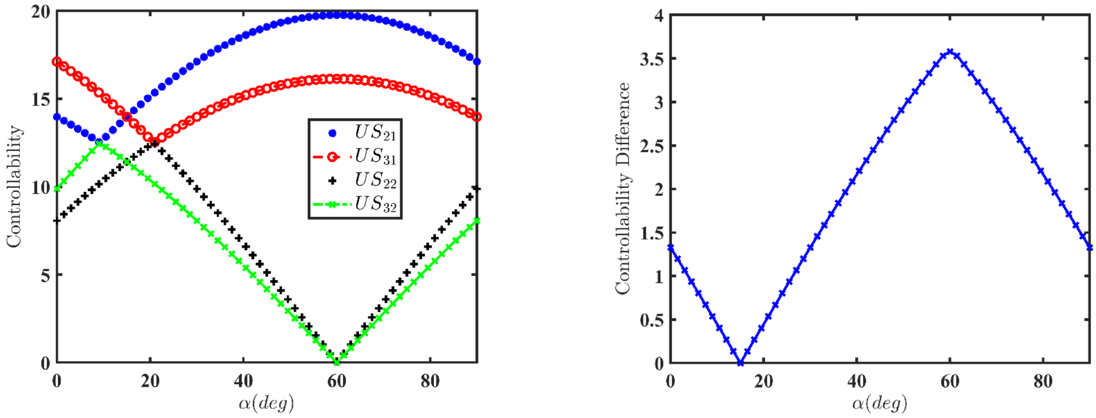

Figure 10. Failure of number two motor

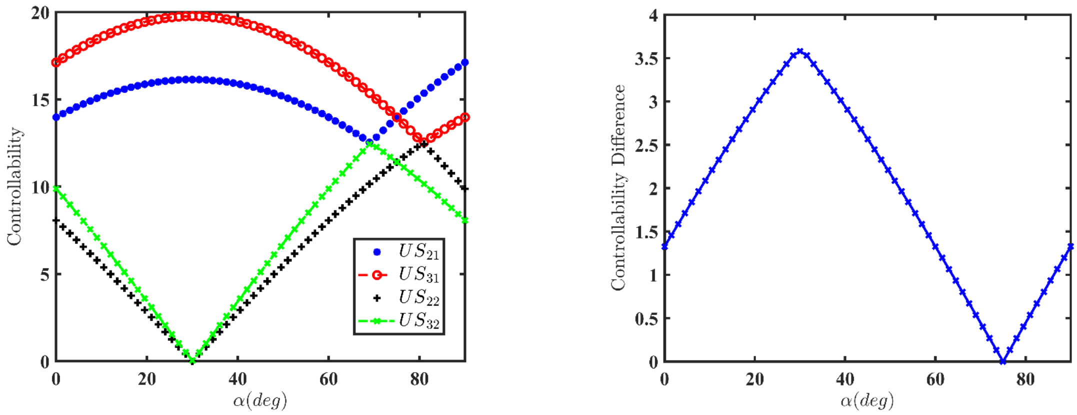

Figure 11. Failure of number three motor

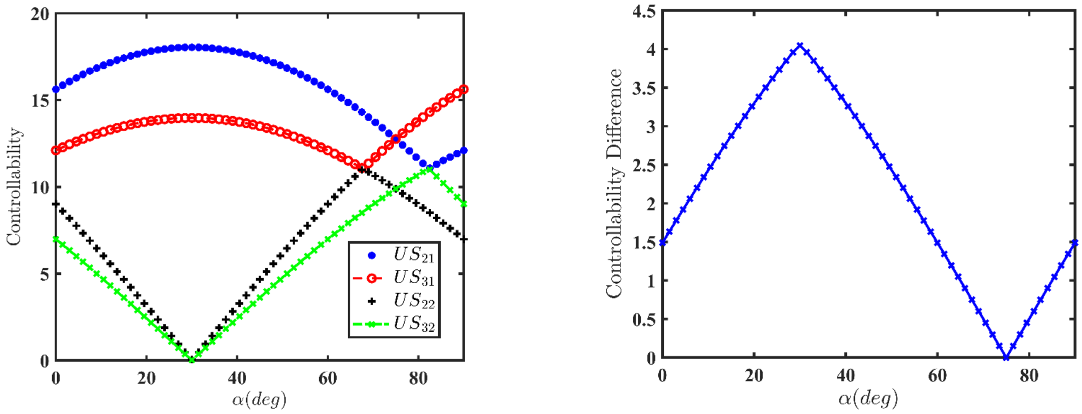

Figure 12. Failure of number one and two motors

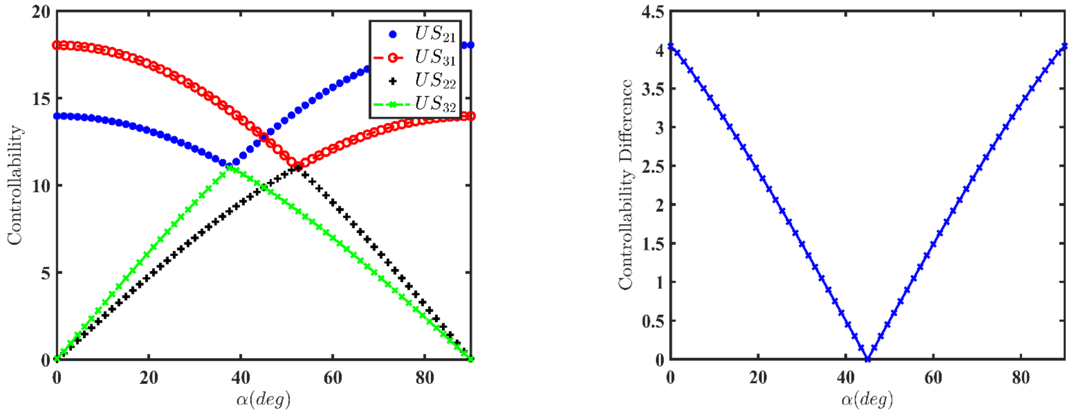

Figure 13. Failure of number two and three motors

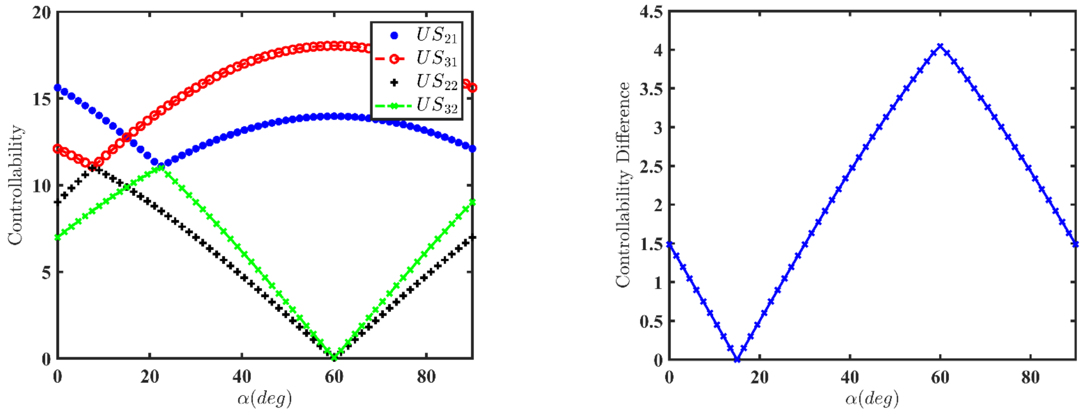

Figure 14. Failure of number three and four motors

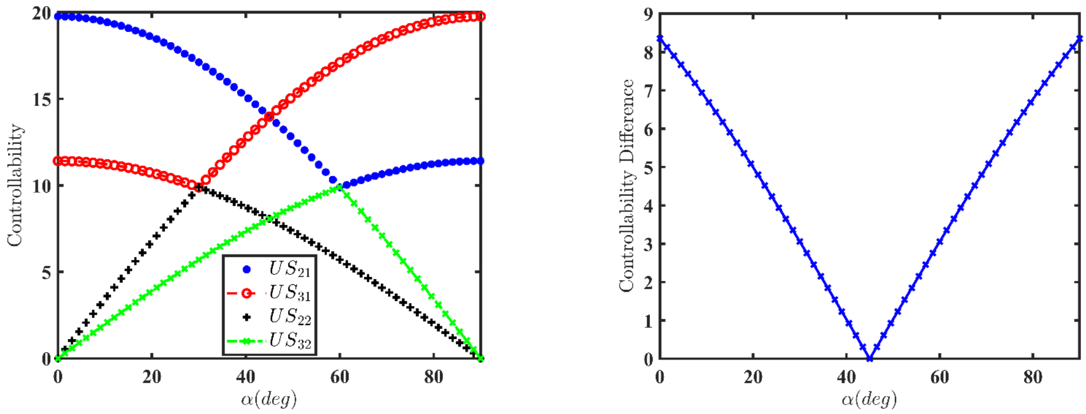

Figure 15. Failure of number one and four motors

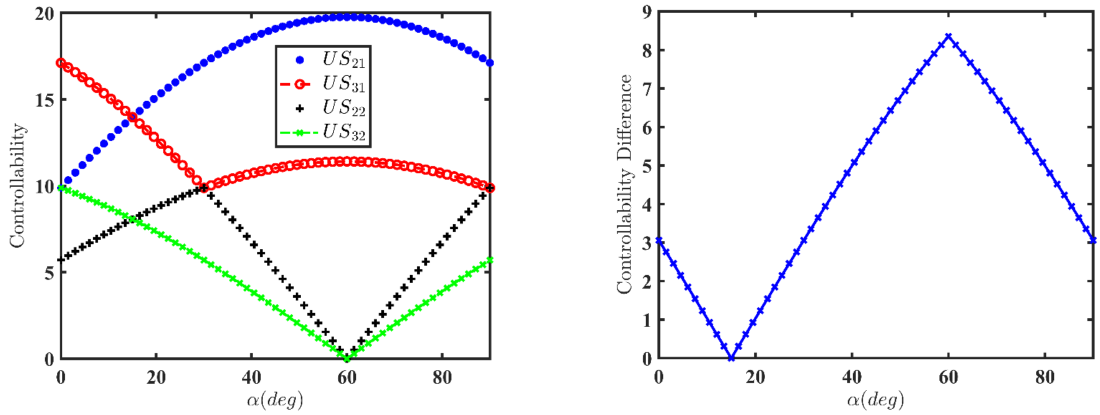

Figure 16. Failure of number two and five motors

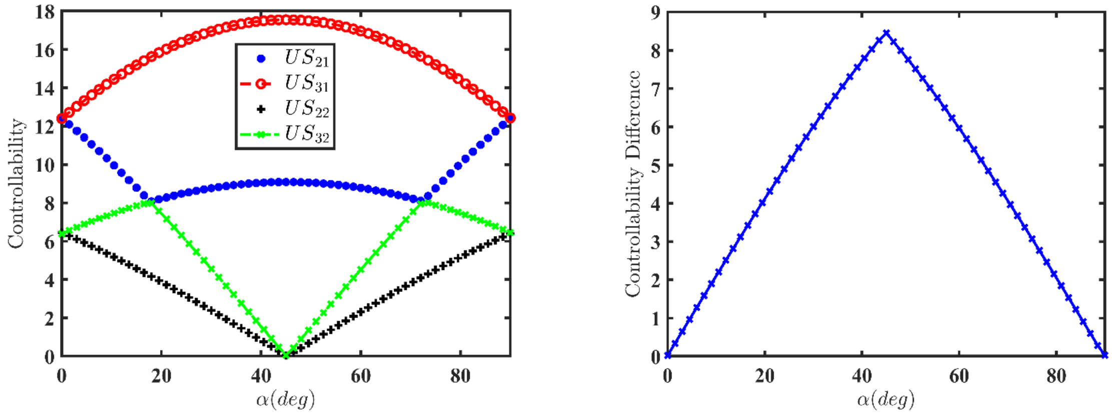

Figure 17. Failure of number one, three, and six motors

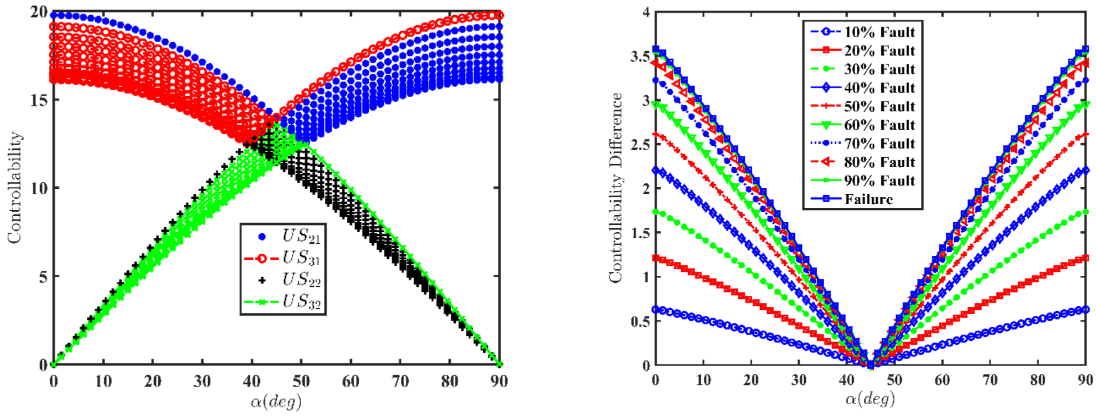

Figure 18. Different magnitudes of fault on number one motor

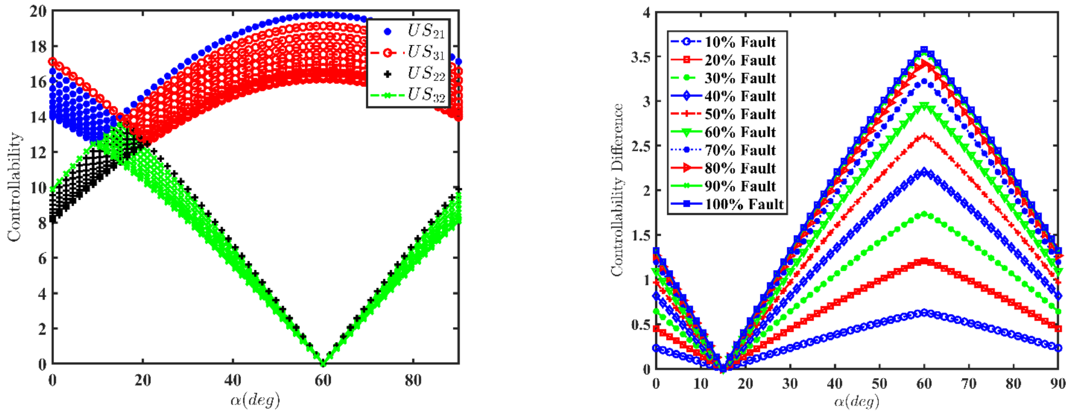

Figure 19. Different magnitudes of fault on number two motors

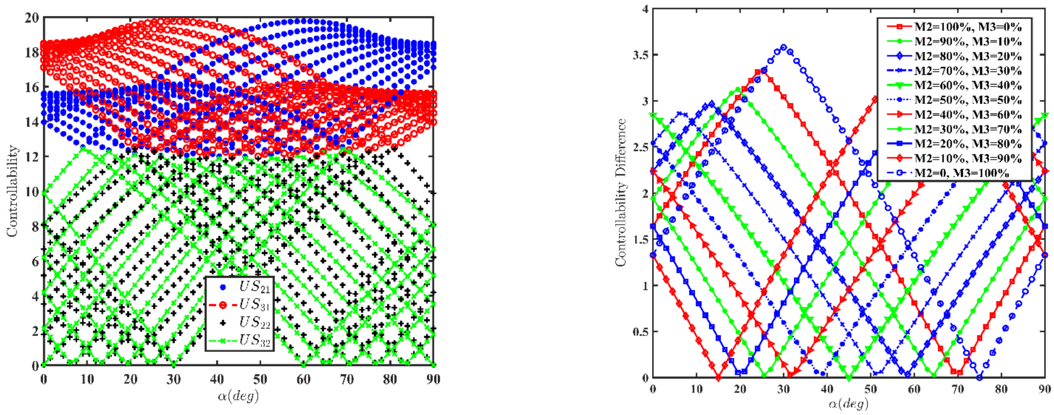

Figure 20. Different magnitudes of fault on number two and three motors

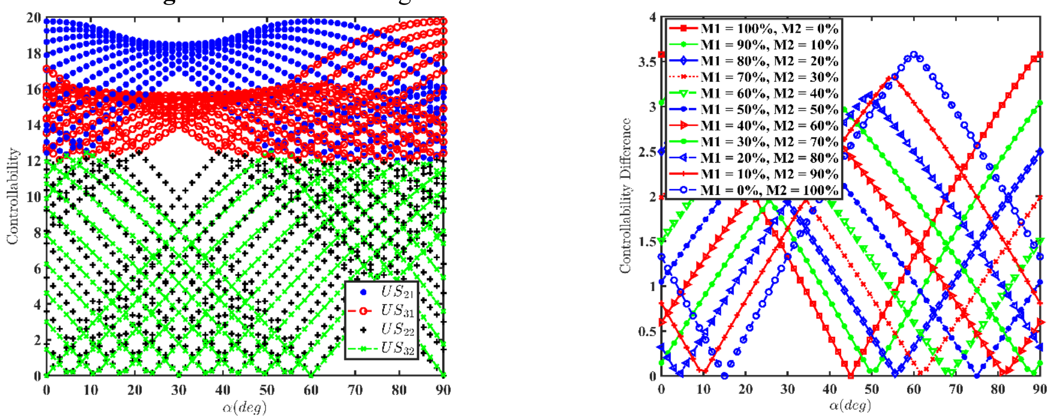

Figure 21. Different magnitudes of fault on number one and two motors

Controlability of multi-rotors under motor fault effect

According to the above discussion, depending on the number of faulty rotors, the optimum angles take place on the angles of 15°,45°, and 75° degrees. The result of the above analysis is all presented in Table 1 as below:

Table 1. Optimum angles for different motor failures of hexarotor

Motor Failure	Optimum angle	Motor Failure	Optimum angle
No. 1	45°	No. 2, 3	45°
No. 2	15°	No. 3, 4	15°
No. 3	75°	No. 1, 4	45°
No. 1, 2	75°	No. 2, 5	15°

5. Conclusion

This paper investigates the effect of different magnitudes of faults and failures on multirotors including the quadrotor and hexarotor. According to the results, quadrotors lose their controllability in presence of motor failure. For different magnitudes of faults, it is demonstrated that the minimum body rotation angle with the minimum difference between controllability around the main axes of the quadrotor is 45°. It means that the quadrotor with cross configuration has better controllability around both axes. Another benefit of the quadrotor with cross-configuration is that pitch and roll maneuver do not induce an unwanted yawing moment on the airframe. Examining the results for hexarotors demonstrate that different fault and failures on different motors result in different minimum angles. It means that depending on the magnitude of fault and the number of faulty rotor, different optimum rotation angles can be reached. For some configurations the optimum angle does not change with the variation of the magnitude of fault, while in some configurations the magnitude of fault alters the optimum angle. Based on the results, depending on the number of faulty rotor, the optimum angles generally occur on the angles of 15, 45, and 75 degrees. The above analysis helps the selection of fault-tolerant control strategy in flight. By knowing the fault and failure on the multirotor using the fault detection algorithm and knowing the best rotation angle according to the paper's results, the body will rotate according to the pre-determined optimum angles and then will continue the flight. Using the above strategy will help to change the configuration to a configuration, which has the minimum difference of controllability around the pitch and roll axes and therefore increase the chance of safe landing in presence of motor failure.

Acknowledgements

This research is supported by the Scientific and Technological Research Council of Turkey (TÜBİTAK) under 3501 programs, with project number [120M793].

Contribution of Authors: DA has developed the theoretical analysis and the numerical simulations as well as manuscript preparation; KA has helped in controllability analysis and simulations, YN has developed the related codes and OT has helped in manuscript writing.

Conflict of Interests: The authors have not conflict of interest to declare.

Research and publication ethic statement: All the developed results presented in this study have been conducted under the strictest ethical guidelines.

References

[1]Turan, V., Avşar, E., Asadi, D., Aydın, E. (2021). Image processing based autonomous landing zone detection for a multi-rotor drone in emergency situations. Turkish Journal of Engineering, 5(4): 193-200.

[2] Asadi, D. (2022). Partial engine fault detection and control of a Quadrotor considering model uncertainty. Turkish Journal of Engineering, 6(2): 106-117.

[3]Asadi, D., Ahmadi, K., Nabavi, S. Y. (2021). Fault-tolerant Trajectory Tracking Control of a Quadcopter in Presence of a Motor Fault. International Journal of Aeronautical & Space Sciences,1-14.

[4] Asadi, D., Atkins E. M. (2018). Multi-objective weight optimization for trajectory planning of an airplane with structural damage. Journal of Intelligent & Robotic Systems. 91(3), 667-690.

[5] Asadi, D., Sabzehparvar, M., Atkins, E. M., and Talebi, H. A. (2014). Damaged airplane trajectory planning based on flight envelope and stability of motion primitives. Journal of Aircraft, 51(6), 1740-1757.

[6] Asadi, D., Sabzehparvar, M., Talebi, H.A. (2013). Damaged airplane flight envelope and stability evaluation. Aircraft Engineering and Aerospace Technology, 85(3),186-198.

[7] Ahmadi, K., Asadi, D., Pazooki, F.(2017). Nonlinear L1 adaptive control of an airplane with structural damage. Proceedings of the Institution of Mechanical Engineers, Part G: Journal of Aerospace Engineering, 233(1), 341-353.

[8] Asadi, D., Ahmadi, K., Nonlinear Robust adaptive control of an airplane with structural damage, Proceedings of the Institution of Mechanical Engineers, Part G: Journal of Aerospace Engineering, 2020. doi:10.1177/0954410020926618.

[9] Asadi, D., Bagherzadeh, S. (2017). Nonlinear adaptive sliding mode tracking control of an airplane with wing damage. Proceedings of the Institution of Mechanical Eng., Part G: Journal of Aerospace Engineering, 232 (8), 1405-1420.

[10] Alwi, H., Edwards, C. (2013). Fault-tolerant control of an octorotor using LPV based sliding mode control allocation. American Control Conference (ACC), 6505–6510.

[11] Navabi, M., Davoodi, A., Mirzaei, H. (2021). Trajectory tracking of under-actuated quadcopter using Lyapunov-based optimum adaptive controller. Proceedings of the Institution of Mechanical Engineers, Part G: Journal of Aerospace Engineering, 1, 1-14.

[12] Ahmadi Dastgerdi, K., Pazooki, F., Roshanian, J. (2020). Model reference adaptive control of a small satellite in the presence of parameter uncertainties. Scientia Iranica, 27(6): 2933-2944.

[13] Asadi, D., Sabzehparvar, M. Talebi, H.A. (2013). Damaged airplane flight envelope and stability evaluation. Aircraft Engineering and Aerospace Technology, 85(3),186-198.

[14] Gao, Z., Cecati, C., Ding, S.X. (2015). A survey of fault diagnosis and fault-tolerant techniques—part I: fault diagnosis with modelbased and signal-based approaches. IEEE Trans Ind Electro 62(6):3757–3767.

[15] Amoozgar, M.H., Chamseddine, A., Zhang, Y. (2013). Experimental test of a two-stage Kalman flter for actuator fault detection and diagnosis of an unmanned quadrotor helicopter. J Intell Robot Syst, 70, 107–117.

[16] Cen, Z., Noura, H., Susilo, B.T., Younes, Y.A. (2014). Robust fault diagnosis for quadrotor UAVs using adaptive Thau observer. J Intell Robot Syst, 73(1–4),573–588 26.

[17] Han. W., Wang, Z., Yi, S. (2018). Fault estimation for a quadrotor unmanned aerial vehicle by integrating the parity space approach with recursive least squares. Proc Inst Mech Eng G, 232(4), 783–796.

[18] Dongjie, S., Binxian, Y., Quan, Q. (2016). Reliability analysis of multicopter configurations based on controllability theory. Proceedings of the 35th Chinese Control Conference July 27-29, Chengdu, China.

[19] Pasqualetti, F., Zampieri, S., Bullo, F. (2014). Controllability metrics, limitations and algorithms for complex networks. IEEE Transactions on Control of Network Systems, 1(1), 40–52.

[20] Lindmark, G., Altafini, C. (2018). Minimum energy control for complex networks. Nature Scientific Reports, 8(1), 1–14.

[21] Chaisena, K., Chamniprasart, K., Tantrairatn, S. (2018). An automatic stabilizing system for balancing a multi-rotor subject to variations in center of gravity and mass. Third International Conference on Engineering Science and Innovative Technology (ESIT), 1-5, doi: 10.1109/ESIT.2018.8665339.

[22] Cutler, M., How, J. P. (2015). Analysis and control of a variable-pitch quadrotor for agile flight. ASME. J. Dyn. Sys., Meas., Control. 137(10): 101002. https://doi.org/10.1115/1.4030676.

[23] Kumar, R., Deshpande, A. M., Wells, J. Z., Kumar, M. (2020). Flight control of sliding arm quadcopter with dynamic structural parameters. 2020 IEEE/RSJ International Conference on Intelligent Robots and Systems (IROS), 1358-1363, doi: 10.1109/IROS45743.2020.9340694.

[24] Driessens, S., Pounds, P. (2015). The triangular quadrotor: a more efficient quadrotor configuration. IEEE Transactions on Robotics, 31(6), 1517-1526.

[25] Magnussen, O., Hovland, G., Ottestad, M. (2014). Multicopter UAV design optimization, in 2014 IEEE/ASME 10th International Conference on Mechatronic and Embedded Systems and Applications (MESA), 1-6.

[26] Lanzon, A., Freddi, A., Longhi, S. (2014). Flight control of a quadrotor vehicle subsequent to a rotor failure. Journal of Guidance, Control, and Dynamics, 37(2), 580–591.

[27] Mueller, M. W., D'Andrea, R. (2014). Stability and control of a quadrocopter despite the complete loss of one, two, or three propellers. Robotics and Automation (ICRA), IEEE International Conference on, 45–52.

[28] Du, G.-X., Quan, Q., and Cai, K.-Y. (2015). Controllability analysis and degraded control for a class of hexacopters subject to rotor failures. Journal of Intelligent & Robotic Systems, 78(1), 143–157.

[29] Giribet, J. I., Sanchez-Pena, R. S., Ghersin, A. S. (2016). Analysis and design of a tilted rotor hexacopter for fault tolerance. IEEE Transactions on Aerospace and Electronic Systems, 52(4) 1555–1567.

[30] Lee, J., Choi, H. S., Shim, H. (2016). Fault-tolerant control of hexacopter for actuator faults using time delay control method. International Journal of Aeronautical and Space Sciences, 17, 54–63.

[31]Fault-tolerant Control Allocation for Multi-rotor Helicopters using Parametric Programming, Thomas Schneider, Guillaume Ducardy, Konrad Rudin, and Pascal Struplerz, Conference: International Micro Air Vehicle Braunschweig, Germany.

[32] Quan, Q. (2017). Introduction to Multicopter Design and Control. Springer, Singapore.

[33] Tahavori, M., Hasan, A. (2020). Fault recoverability for nonlinear systems with application to fault-tolerant control of UAVs. Aerospace Science and Technology, 107. 10.1016/j.ast.2020.106282.

[34] Gupta, R., Zhao, W., Kapania, R. K. (2020). Controllability gramian as control design objective in aircraft structural design optimization. AIAA Journal, 58(7), 3199–3220. https://doi.org/10.2514/1.J059102.